

# Superstatistical analysis of sea-level fluctuations

Pau Rabassa and Christian Beck

*School of Mathematical Sciences, Queen Mary University of London, Mile End Road, London E1 4NS, UK*

We perform a statistical analysis of measured time series of sea levels at various coastal locations in the UK, measured at time differences of 15 minutes over the past 20 years. When the astronomical tide and other deterministic components are removed from the record, a stochastic signal corresponding to the meteorological component remains, and this is well-described by a superstatistical model. We do various tests on the measured time series, and compare the data at 5 different UK locations. Overall the  $\chi^2$ -superstatistics is best suitable to describe the data, in particular when one looks at the dynamics of sea-level *differences* on short time scales.

Keywords: Superstatistics, Sea levels, Data analysis, Surges, Non-tidal residuals

## I. INTRODUCTION

Many complex nonequilibrium phenomena can be understood as the superposition of different dynamics on different time scales. The superstatistical approach [1] models these complex phenomena as the superposition of two random variables, one that corresponds to local equilibrium statistical mechanics and another one that corresponds to a slowly varying parameter  $\beta$ , which for example can be the local inverse temperature in a spatio-temporal inhomogeneous system, or some local variance parameter associated with slices of a given size in a given time series. In nonequilibrium statistical mechanics, this technique is a powerful tool to describe a large variety of complex systems for which there is a spatial or temporal change of conditions on a large scale, larger than the local relaxation time [2–10]. Effectively, when integrating out the fluctuations of the parameter, this leads to more general types of statistical mechanics, described by more general entropy functions [10–12]. Essential for superstatistical models is sufficient time scale separation, i.e. the local relaxation time of the system must be much shorter than the typical time scale on which the parameter  $\beta$  changes. Many interesting applications of the superstatistics concept have been worked out for a variety of complex systems, for example the analysis of train delay statistics [13], hydrodynamic turbulence [14], cancer survival statistics [15] and much more [16–21]. Typical distributions of the superstatistical parameter  $\beta$  that occur in many of these applications are the  $\chi^2$ , inverse  $\chi^2$  or lognormal distribution [2]. Superstatistics based on  $\chi^2$  distributions leads to  $q$ -statistics [11, 22], whereas other distributions lead to more complicated versions of generalized statistical mechanics [10].

Of particular interest are superstatistical techniques to analyse and model the complexity inherent in environmental time series, such as rainfall, wind, surface temperature, and related quantities. Rapisarda et al. [19] and Kantz et al. [23] investigated superstatistical aspects of wind velocity fluctuations. Yalcin et al. [24] did a data analysis of relevant surface temperature distributions on the earth, which is important if one wants to understand the effective statistical mechanics for thermodynamic devices (or local ecosystems) that are kept in the open air outside a constant-temperature environment. Porporato et al. [25] looked at rainfall statistics and developed a model where the rate parameter of the underlying Poisson process fluctuates in a superstatistical way.

A central point for the applicability of the superstatistics concept is the existence of suitable time scale separation of the dynamical evolution, or more generally the existence of a hierarchy of time scales which are well separated. In the simplest case this just means there are two different time scales such that the typical variation of  $\beta$  takes place on a much larger time scale than the local relaxation time of the system that is influenced by the given temperature environment. There are tests that can check for a given experimental time series if such a time scale separation is present [8].

In this paper we will deal with a new application of the superstatistics concept that has not been considered before, namely the superstatistical analysis of measured sea-level fluctuations at various spatial locations in the UK. Of particular interest is: a) which type of superstatistics is relevant for sea levels; b) how the results differ from spatial location to location; c) how well the time scale separation criterium is satisfied and d) what the relevant time scales are. Our data set consists of a record of measured sea levels at various tide gauge locations in the UK that were measured every 15 minutes over the past 20 years or so. In Section II we review the derivation and application of

the superstatistical approach and the different tools to check its suitability for a particular data set, in our case sea-level data. In Section III we analyse the data set of observed sea levels at five different sites in the United Kingdom, and provide answers to questions a)–d). Our concluding remarks are given in section IV.

## II. SUPERSTATISTICAL ANALYSIS OF TIME SERIES.

### A. The superstatistical model

Consider a stochastic process that for a short frame of time is well described by a Gaussian distribution, but on a longer time scale the parameter value  $\beta$  of this Gaussian fluctuates. Concretely, for a given value of  $\beta$  the conditional probability distribution is given by

$$p(v|\beta) \sim \exp\left(-\frac{\beta v^2}{2}\right).$$

Assume that there exists a probability distribution  $f(\beta)$  describing the fluctuations of  $\beta$ , then the density function is expected to behave as

$$p(v) = \int_0^\infty f(\beta)p(v|\beta)d\beta \sim \int_0^\infty f(\beta)e^{-\beta v^2/2}d\beta. \quad (1)$$

There are three different superstatistics distributions which are commonly found in many applications:

**$\chi^2$ -superstatistics**, also known as Tsallis statistics. The function  $f(\beta)$  is given by the  $\Gamma$ -distribution

$$f(\beta) = \frac{1}{\Gamma\left(\frac{n}{2}\right)} \left(\frac{n}{2\beta_0}\right)^{n/2} \beta^{n/2-1} e^{-n\beta/2\beta_0},$$

where  $\beta_0$  is the average of  $\beta$  and  $n$  is the number of degrees of freedom.

**Inverse  $\chi^2$ -superstatistics.** In this case  $f(\beta)$  is given by the inverse  $\Gamma$ -distribution

$$f(\beta) = \frac{\beta_0}{\Gamma\left(\frac{n}{2}\right)} \left(\frac{n\beta_0}{2}\right)^{n/2} \beta^{-n/2-2} e^{-n\beta_0/2\beta},$$

where  $\beta_0$  is again the average of  $\beta$  and  $n$  is the number of degrees of freedom of the inverse  $\chi^2$  distribution.

**Lognormal superstatistics.** In this last case  $f(\beta)$  is described by the lognormal distribution

$$f(\beta) = \frac{1}{\sqrt{2\pi s\beta}} \exp\left(-\frac{\left(\ln\frac{\beta}{\mu}\right)^2}{2s^2}\right),$$

where  $\mu$  and  $s$  are suitable parameters.

### B. Tools for data analysis

Consider  $u = \{u_1, \dots, u_n\}$  as a set of  $n$  experimental observations (or data points in general). The total time series is divided into  $N$  slices of length  $\Delta$ , with  $N = \lfloor n/\Delta \rfloor$  where  $\lfloor \cdot \rfloor$  denotes the integer part (or floor) function. The local moment of order  $k$  (of the  $l$ -th slice) is then defined as:

$$\langle u^k \rangle_{\Delta, l} = \frac{1}{\Delta} \sum_{j=1+(l-1)\Delta}^{l\Delta} u_j^k, \text{ with } l = 1, 2, \dots, N.$$

In the following, we will assume that the first moment of the total time series is zero ( $\langle u \rangle_{n,1} = 0$ ).

*Computation of time scales*

A physical process that is well modeled by a superstatistics has two different time scales. The short time scale  $\tau$  corresponds to the time that it takes for the system to get to local equilibrium. The long time scale  $T$  corresponds to the time scale that the system remains in local equilibrium before it fluctuates to another phase state with a different  $\beta$ .

Given a time series generated by a superstatistical process, the autocorrelation function should decay exponentially on a short time scale  $\tau$  (see [2]). In other words

$$C_{n,\tau}(u) = e^{-1}C_{n,0}(u), \quad (2)$$

where  $C_{n,t}(u)$  is the autocorrelation function of the time series  $u$  defined as

$$C_{n,t}(u) = \frac{1}{n-t} \sum_{i=1}^{n-t} u_i u_{i+t}.$$

Assume that we have our data divided into  $N$  slices of length  $\Delta$  as before. We can consider the local averaged kurtosis associated to that length

$$\kappa_{\Delta} := \frac{1}{N} \sum_{l=1}^N \kappa_{\Delta,l}, \quad \text{with } \kappa_{\Delta,l} = \frac{\langle u^4 \rangle_{\Delta,l}}{\langle u^2 \rangle_{\Delta,l}^2}. \quad (3)$$

The long time scale  $T$  corresponds to the optimal time scale for which the process is best described as a superposition of Gaussian random variables. The choice proposed in [2] is to take  $T$  such that

$$\kappa_{\Delta} = 3. \quad (4)$$

This choice has been found to work well for a variety of experimental data [2, 8].

*An additional constraint*

Besides the existence of two separated timescales, it is also necessary to check that the Gaussian hypothesis used to derive the model is satisfied. Assume that we have found the value of  $\Delta$  for which  $\kappa_{\Delta} = 3$ ; we denote it by  $T$ . The original time series is divided into  $N = \lfloor n/T \rfloor$  slices of length  $T$ . Let  $\langle u^2 \rangle_{T,l}$  and  $\langle u^4 \rangle_{T,l}$  denote the second and the fourth moments of these time slices. Consider the value  $\kappa_{\Delta}$  defined by (3) for  $\Delta = NT$ . For large data series,  $\kappa_{NT}$  is a good approximation of  $\kappa_{n,1}$  (the kurtosis of the complete data set) because  $N = \lfloor n/T \rfloor \approx n/T$ . Moreover,  $\kappa_{NT}$  can be expressed as follows:

$$\kappa_{NT} = \left( \frac{1}{N} \sum_{j=1}^N \langle u^2 \rangle_{T,j} \right)^{-2} \frac{1}{N} \sum_{j=1}^N \langle u^4 \rangle_{T,j} \quad (5)$$

In the case that the data in each of these time slices are distributed exactly like a Gaussian random variable (with zero mean and variance  $1/\beta_{\Delta,l}$ ), then the first four local moments are

$$\langle u \rangle_{T,j} = 0, \quad \langle u^2 \rangle_{T,j} = \frac{1}{\beta_{\Delta,j}}, \quad \langle u^3 \rangle_{T,j} = 0, \quad \langle u^4 \rangle_{T,j} = \frac{3}{\beta_{\Delta,j}^2}.$$

In the case where the data in each of these time slices is approximately distributed like a Gaussian random variable, we expect the moments to be close to the ones above. Let  $\theta_{T,l}$  be the deviation of the fourth moment  $\langle u^4 \rangle_{T,l}$  from  $3\langle u^2 \rangle_{T,l}^2$  for the  $l$ -th time slice of length  $T$

$$\theta_{T,l} = \langle u^4 \rangle_{T,l} - 3\langle u^2 \rangle_{T,l}^2.$$

The approximate kurtosis (5) can be rewritten as:

$$\kappa_{NT} = \left( \frac{1}{N} \sum_{j=1}^N \langle u^2 \rangle_{T,j} \right)^{-2} \frac{1}{N} \sum_{j=1}^N [3\langle u^2 \rangle_{T,j}^2 + \theta_{T,j}].$$

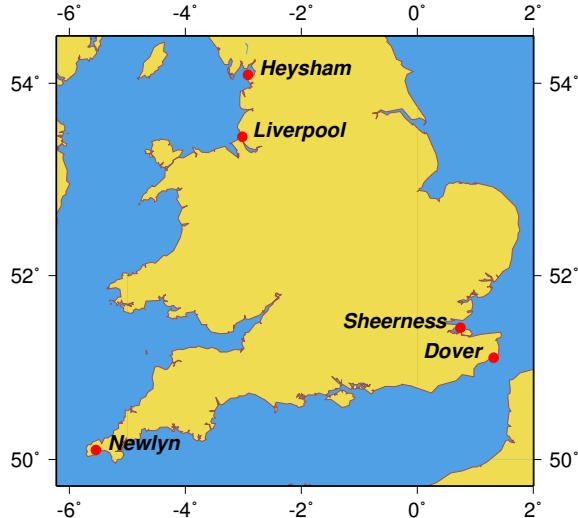


FIG. 1: Geographic locations of sea level gauge stations considered.

Gauge location	Recorded	Missing	Completeness
Dover	640225	61055	91.29%
Heysham	562896	138384	80.27%
Liverpool	616066	85214	87.85%
Newlyn	654818	46462	93.37%
Sheerness	526026	175254	75.01%

TABLE I: Complementary information to the analysed data. We have the number of satisfactorily recorded observations, the number of missing observations and the % of completeness for each site.

When the Gaussian approximation is reasonable, the contribution of the terms  $\theta_{T,j}$  to  $\kappa_{NT}$  is small as compared to the terms  $3\langle u^2 \rangle_{T,j}^2$ . Consider the parameter  $\epsilon$  given as

$$\epsilon = \frac{1}{3} \frac{\sum_{j=1}^N \theta_{T,j}}{\sum_{j=1}^N \langle u^2 \rangle_{T,j}^2}. \quad (6)$$

This parameter measures the contribution of the deviations from the Gaussian approximation in these time slices to the value of  $\kappa_{n,1}$ . Concretely, we expect the local Gaussian approximation to hold for a given time series when  $|\epsilon|$  is small. For more details see [8].

### III. ANALYSIS OF THE SEA LEVEL DATA

#### A. Nature of the sea level data

In this paper we analyse observed sea level data available from the British Oceanographic Data Centre [39]. Our study focusses on recorded sea levels from the UK Tide Gauge Network at five particular locations: Dover, Heysham, Liverpool, Newlyn and Sheerness. These locations have been selected for our analysis as a representative subset out of a network of 45 different sites. The map in Figure 1 shows the geographical locations of these five gauge stations.

The data at each location is composed of one observation every quarter of hour from the 1st of January 1993 to the 31st of December 2012. The data is processed and quality-controlled by the British Oceanographic Data Center. Each satisfactory recorded sea level value is also provided with a corresponding value of the non-tidal residual (see below for details). Table I displays some

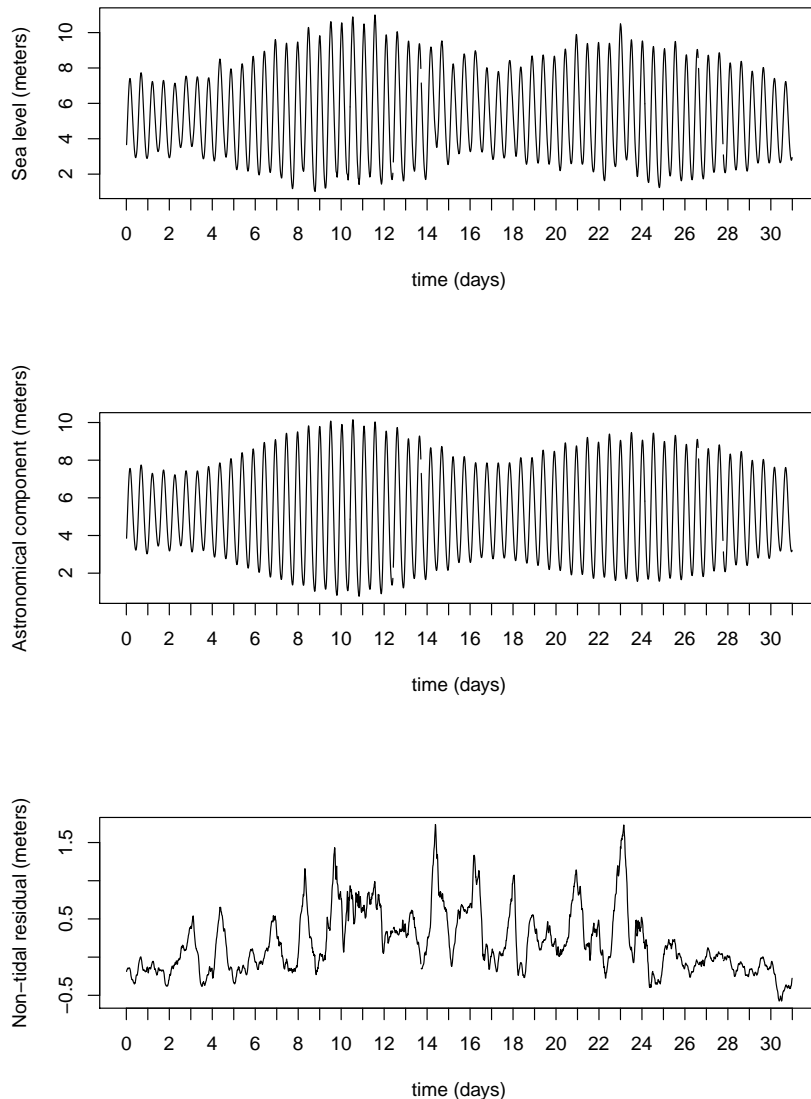


FIG. 2: Sea-Level time series at Heysham in January 1993. Top: observed sea level  $Z(t)$ . Middle: astronomical tide  $X(t)$ . Bottom: Non-tidal residual  $Y(t)$ .

background information on the number of data recorded in a satisfactory way at each site for the time period considered.

The observed sea level  $Z(t)$  (at a given time  $t$ ) is typically decomposed into three different components [26]

$$Z(t) = M(t) + X(t) + Y(t),$$

which are the following:

**Annual mean sea level** ( $M(t)$ ). On a local scale its temporal changes are the product of a couple of (inherently coupled) processes such as volume and mass changes due to (i) exchange of water with the atmosphere and the continents and (ii) mass redistribution due to changing winds and sea level pressure [27–30], and vertical land motion [32, 33]. These variations vary locally and can be as large as  $\sim \pm 80\text{cm}$  on an inter-monthly or  $\sim \pm 50\text{cm}$  on an inter-annual

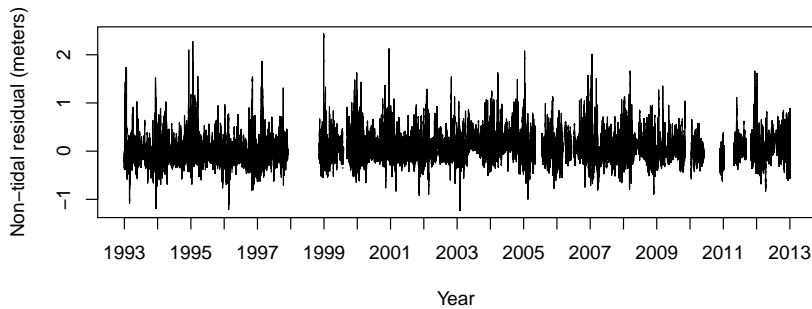


FIG. 3: Available non-tidal residual  $Y(t_i)$  at Heysham from 1 January 1993 to 31 December 2012.

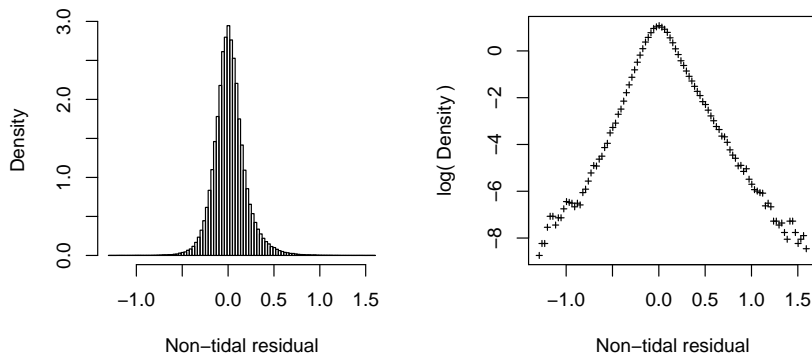


FIG. 4: Histogram of non-tidal residuals at Dover (in a logarithmic scale at the left).

time scale. Additionally there is a secular long-term trend of the mean sea level from 1 to 3mm/year [34, 35]. Given a set of observations at a particular site, it can be determined by simple regression and removed from the data.

**The astronomical tide ( $X(t)$ ).** This is the non-stochastic part of the sea-level change that is caused by the changing forces of moving planetary objects. This component is modelled as the sum of  $m$  different tidal constituents [36]:

$$X(t) = \sum_{i=1}^m H_i \cos(\omega_i t + \phi_i).$$

The angular frequencies  $\omega_i$  and the number of constituents  $m$  are fixed, whereas the amplitudes  $H_i$  and the phase lags  $\phi_i$  can be computed from the data on every site.

**Non-tidal residual ( $Y(t)$ ).** This component primarily contains the meteorological contribution to sea level often termed the surge, which has stochastic behaviour. This component can be also influenced by tide-surge interaction, harmonic prediction error, gauge timing error, tide-river flow interaction, etc.; see [37] and references therein.

In Table II we have included the cross-correlation matrix associated with observed non-tidal residual levels at the different locations. We can observe that there is some correlation between the locations that are geographically close to each other (see Figure 1), Dover correlated with Sheerness

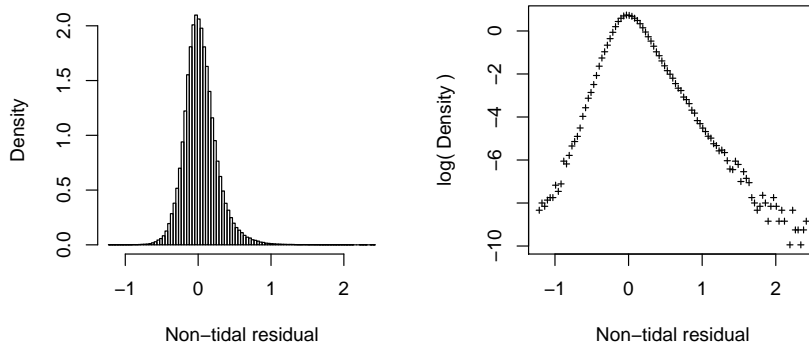


FIG. 5: Histogram of non-tidal residuals at Heysham (in a logarithmic scale at the left).

	Dover	Heysham	Liverpool	Newlyn	Sheerness
Dover	1.000	0.061	0.112	0.144	0.745
Heysham		1.000	0.885	0.412	-0.257
Liverpool			1.000	0.379	-0.242
Newlyn				1.000	0.016
Sheerness					1.000

TABLE II: Correlation matrix for non-tidal residuals at five different tide gauges in the UK.

and Heysham correlated with Liverpool, whereas there is only little correlation between distant sites.

Figure 2 displays the observations at Heysham in January 1993. The figure also shows the deterministic astronomical tide (middle panel) and the non-tidal residual (bottom panel) for one month. The non-tidal residual for the whole 20-year period is shown in Figure 3.

Our analysis focusses on determining if the observed non-tidal residual  $Y(t)$  is well fitted by a superstatistical process. We can observe in Table I and Figures 2 and 3 that the dataset is far from complete, there are both some single observations missing and long periods of time without data. For practical purposes, we will consider only the available data and ignore all the missing values, which are due to mechanical problems with the tide gauge. Therefore our data set will comprise the values for which  $Y(t_i)$  is available.

Figures 4 and 5 show the histograms of recorded non-tidal residuals at Dover and Heysham, respectively. The distributions are non-Gaussian and have fat tails. Some skewness can also be observed in both cases (see also Table III). This is mainly due to the presence of the coast, where the water is piled up, which is not the case if the winds push the water away from the coast. This makes positive surges more extreme than negatives ones, producing a skewed distribution. For more details on the processes contributing to the surge generation in the region see [28, 30, 31] and references therein.

## B. Analysis of the non-tidal residual

In order to determine if a data set can be well modeled by a superstatistics based on locally Gaussian distributions with fluctuating variance, one should check that certain conditions are fulfilled. The first one is that the data has suitable high order moments. Skewness should be close to 0 and kurtosis should be greater than 3. The second condition is to check that there exists a proper time-scale separation. The short time scale  $\tau$  corresponds to the time that it takes for the system

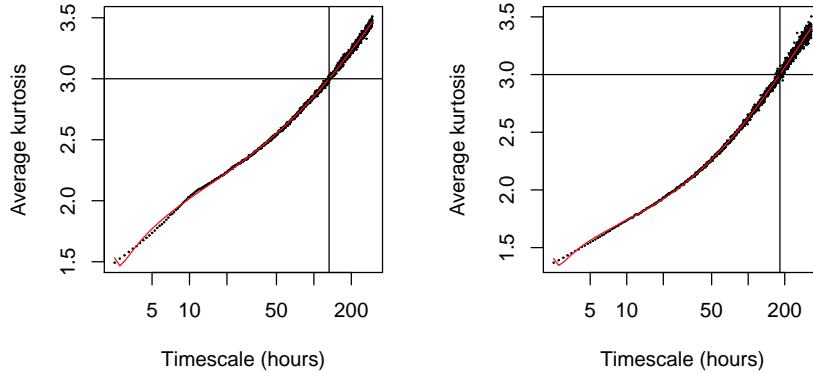


FIG. 6: Computation of optimal time scale  $T$  for observed non-tidal residuals at Dover (left) and Heysham (right). Every dot corresponds to a value of the average kurtosis  $\kappa_{\Delta}$  given by (3). The red line is a polynomial function of degree 5 that best fits the data points. The optimal time scale is obtained as the intersection of this line with  $\kappa = 3$ .

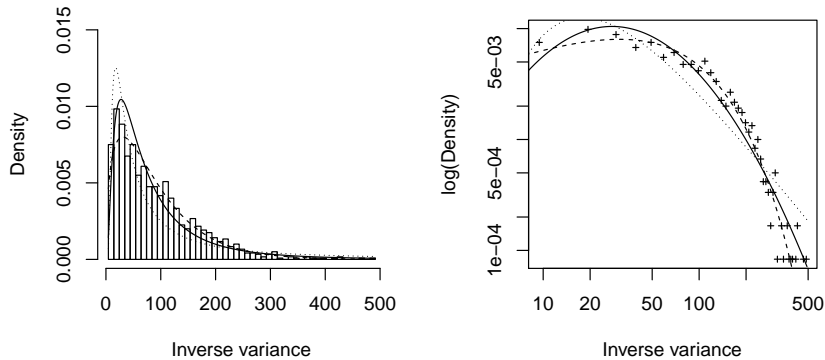


FIG. 7: Probability density  $f(\beta)$  extracted from the non-tidal residuals at Dover and compared to log-normal (solid line),  $\chi^2$  (dashed line) and inverse- $\chi^2$  (dotted line). Left: linear-linear scale, right: log-log scale. All distributions have the same mean and variance as the experimental data.

to get to local equilibrium. It can be computed from the data using eq. (2). The long time scale  $T$  corresponds to the time scale that the system remains in local equilibrium before it fluctuates to another state with different  $\beta$ . This time scale can be computed as the particular value of  $\Delta$  such that eq. (4) holds (see Figure 6). The ratio between the short time scale  $\tau$  and the long time scale  $T$  should be small enough in order to have a proper time scale separation. The third condition to check is that the local Gaussian approximation is a reasonable hypothesis. This corresponds to checking that the parameter  $\epsilon$  given by eq. (6) is close to zero.

Once the optimal time scale  $T$  has been determined one can extract the empirical distribution function  $f(\beta)$  that defines the superstatistical model (1). For this empirical distribution one can determine which of the three universality classes described in Section II A fits the data best. One possibility is to do this just by visual inspection of the fitted distributions [2, 8], but that has the inconvenience of being tedious, especially when applied to multiple datasets or when the parameter space is higher-dimensional. Moreover the visual analysis can be subjective and sometimes it can



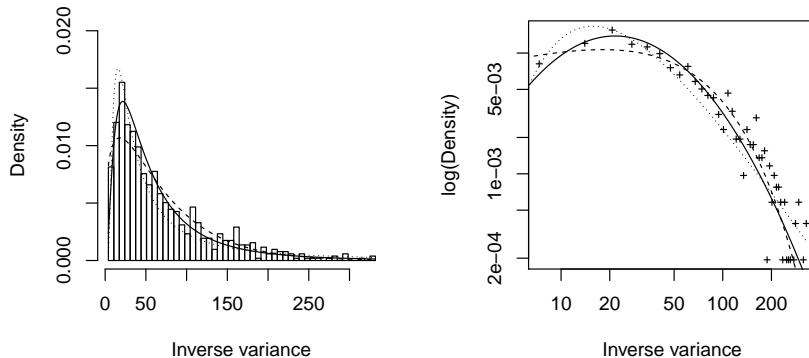


FIG. 8: As Figure 7 but for non-tidal residuals at Heysham.

Location	$\tau$	$T$	$\tau/T$	$ \epsilon $	Skewness	Kurtosis	K-S Distance		
							log-norm.	$\chi^2$	Inv- $\chi^2$
Dover	13.5	132.5	0.10	0.08	0.58	6.68	0.062	0.032	0.169
Heysham	53.25	182.5	0.29	0.13	0.86	6.32	0.035	0.041	0.117
Liverpool	53	169.75	0.31	0.16	0.96	6.77	0.057	0.030	0.138
Newlyn	104.25	998	0.10	0.04	0.54	3.91	0.039	0.048	0.066
Sheerness	9	83.75	0.11	0.13	0.24	9.42	0.057	0.033	0.236

TABLE III: Relevant statistical parameters for applicability of the superstatistical model to observed non-tidal residuals at different locations. The short and the long time scales ( $\tau$  and  $T$ ) are expressed in hours. Parameters  $\tau$ ,  $T$  and  $\epsilon$  are described in Section II B.

be difficult to tell which distribution fits best (see Figures 7 and 8). As a more systematic method we here consider the Kolmogorov-Smirnov (K-S) distance as an objective criterium to determine the best fit. The K-S distance measures the difference between the empirical distribution and the proposed one [38]. Given  $u = \{u_1, \dots, u_n\}$ , a set of observations, its empirical distribution is defined as  $F_n(v) = \frac{1}{n} \sum_{i=1}^n I_{u_i \leq v}$ , where  $I_{u_i \leq v}$  is the indicator function, equal to 1 if  $u_i \leq v$  and equal to 0 otherwise. Given a cumulative distribution function  $F$ , the K-S distance associated to the dataset  $u$  is defined as

$$D_n = \sup_v |F_n(v) - F(v)|.$$

In Table III we show the results of our analysis, i.e. the time scale parameters  $\tau$  and  $T$ , the parameter  $\epsilon$  defined in eq. (6), the kurtosis and skewness of the histogram of the entire signal, as well as the K-S distance of our superstatistical fits, for the five different sites considered. The time scale separation is not very strong, but it is present. The values of  $|\epsilon|$  are in general small for all sites which indicates that the local Gaussian approximation is reasonable. The kurtosis value is always greater than 3 for the entire time series. The parameter that disagrees the most with the hypothesis of simple Gaussian local behavior is the skewness of the data. The data is skewed due to the non-symmetric nature of the storm surges, whereas the superstatistical model in its simplest form is deduced as the superposition of normal random variables which are not skewed. Of course one can consider locally non-symmetric correction terms to the Gaussian, as done e.g. in [40]. However, this introduces an additional fitting parameter to recover the skewness. We avoid this problem in the next section by considering the dynamics of temporal changes of the non-tidal residual instead of the residual itself.

Finally we observe that the K-S distance does not show uniquely which distribution fits the data best. For all locations the empirical distribution  $f(\beta)$  is reasonably well fitted by either a lognormal

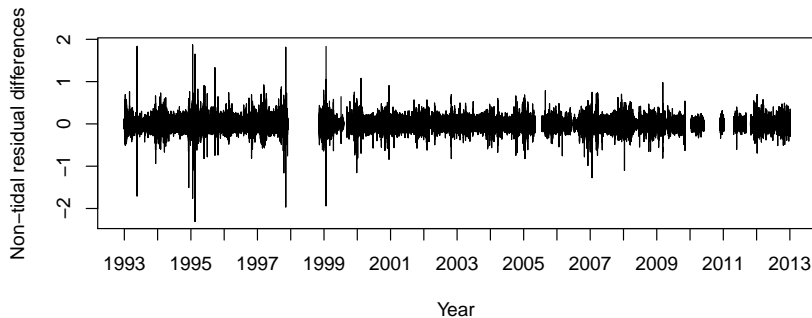


FIG. 9: Available non-tidal residual differences  $Y(t_{i+1}) - Y(t_i)$  at Heysham from 1 January 1993 to 31 December 2012.

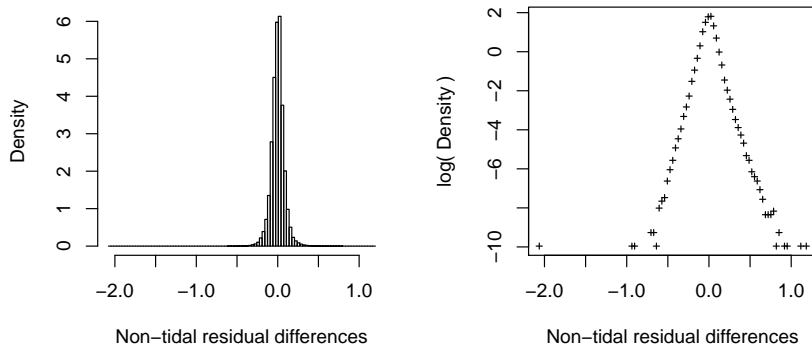


FIG. 10: Histogram non-tidal residual differences at Dover (in a logarithmic scale at the left).

or a  $\chi^2$  distribution, but there is not a clear favourite (see also Figures 7 and 8).

### C. Analysis of non-tidal residual differences

In the previous section we applied the superstatistical analysis directly to the non-tidal residual but we encountered with the problem that the skewness of the data disagrees with the underlying hypothesis of the simplest superstatistical model, which is based on local Gaussian behavior.

Similar as in hydrodynamic turbulence, where one often considers velocity *differences* rather than velocities itself as the relevant quantities, let us therefore look at the differences of observed non-tidal residuals,  $Y(t_{i+1}) - Y(t_i)$ , instead of the residuals  $Y(t_i)$  themselves. Figure 9 displays the available data at Heysham. Figures 10 and 11 display the histogram of differences at Dover and Heysham respectively.

In Table IV we show all relevant parameters for the superstatistical analysis of non-tidal residual differences. We can observe that the data is no longer skewed and the kurtosis is still bigger than 3, as it should be for the entire time series. In all cases except Dover the ratio  $\tau/T$  is smaller than in Table III, which implies that the time scale separation is stronger in this case. On the other hand, the parameter  $|\epsilon|$  is in general bigger but it is still acceptable. Cases like Heysham, where the parameter  $|\epsilon|$  is relatively big, are somewhat exceptional. In [8] it was shown that the presence of outliers in the data set causes  $|\epsilon|$  to grow. The data set considered here may contain measurement

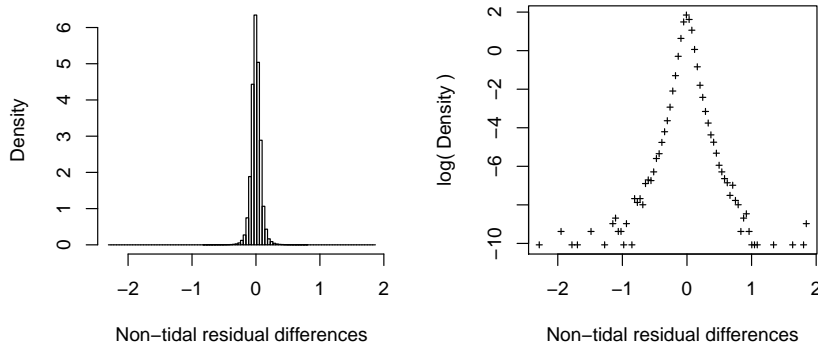


FIG. 11: Histogram of non-tidal residual differences at Heysham (in a logarithmic scale at the left).

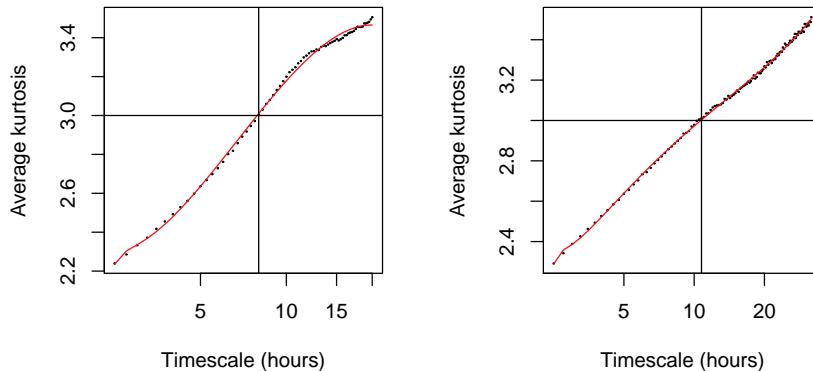


FIG. 12: As Figure 6 but for non-tidal residual differences instead of residuals.

errors. Due to the continuous nature of the sea-level variation, each observation in the data set should be close to the previous one, but possible errors in the data are magnified when considering the difference between sea levels. We believe that this could be a reason why the parameter  $|\epsilon|$  is generally bigger than in the previous case. But further analysis is needed to clarify why the Heysham data generate particularly big  $\epsilon$ .

Our analysis summarized in Table IV shows that  $\chi^2$ -superstatistics is best suited to model the empirical distribution of sea-level changes, better than inverse  $\chi^2$ -superstatistics or lognormal superstatistics, see also Figures 13 and 14. This means that on a long time scale  $q$ -statistics is a good description of the data, and thus the corresponding probability densities maximize  $q$ -entropies [11, 22]. Note that the only case where  $\chi^2$  superstatistics appears to be not the best model (Dover) is also the case with the weakest time scale separation.

#### IV. CONCLUSION

In this paper we have analyzed time series of measured sea level heights for different locations in the UK. While there are minor differences for different locations, the overall picture is that the stochastic component of sea-level changes is well-described by a superstatistical model of  $\chi^2$ -

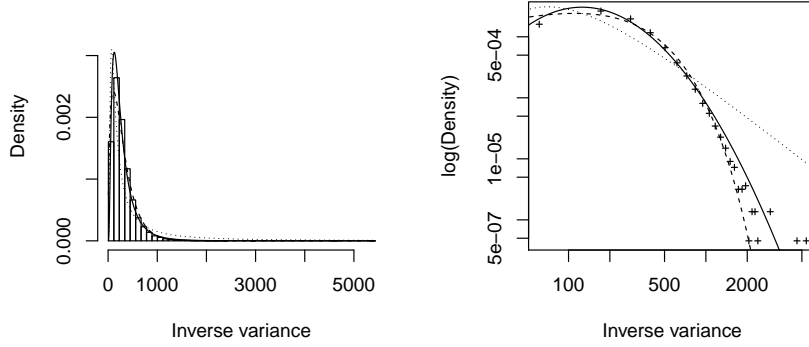


FIG. 13: Probability density  $f(\beta)$  extracted from the non-tidal residual differences  $Y(t_{i+1}) - Y(t_i)$  at Dover and compared to log-normal (solid line),  $\chi^2$  (dashed line) and inverse- $\chi^2$  (dotted line). Left: linear-linear scale, right: log-log scale. All distributions have the same mean and variance as the experimental data.

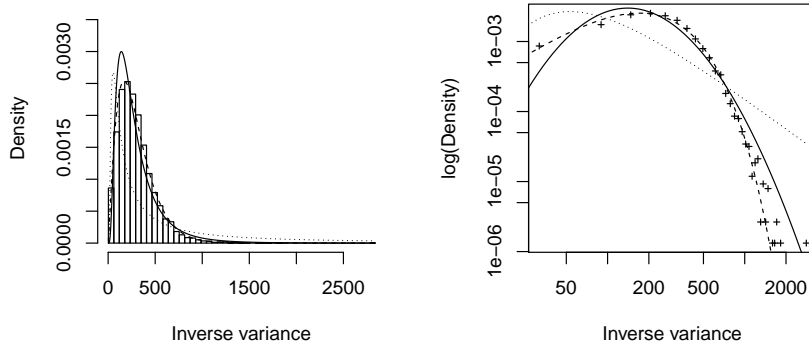


FIG. 14: As Figure 13 but for non-tidal residual differences at Heysham.

type. This type of behavior is different from e.g. fully developed hydrodynamic turbulence, which is better described by lognormal superstatistics [2], or wind velocity fluctuations, described by inverse  $\chi^2$  superstatistics [19, 23]. In future work one might aim to develop a generalized statistical mechanics for the complex behavior of these types of observables in complex environmental systems. A generalized statistical mechanics to describe the statistics of sea levels would thus need to be based on  $\chi^2$  superstatistics (effectively leading to  $q$ -statistics), as shown in this paper by careful analysis of the available data.

Location	$\tau$	$T$	$\tau/T$	$ \epsilon $	Skewness	Kurtosis	K-S Distance		
							log-norm.	$\chi^2$	Inv- $\chi^2$
Dover	1	8	0.125	0.12	0.10	7.61	0.033	0.051	0.212
Heysham	0.75	10.75	0.070	0.72	0.01	16.31	0.060	0.020	0.363
Liverpool	0.75	11.75	0.064	0.34	-0.17	12.81	0.063	0.018	0.367
Newlyn	0.25	13.5	0.018	0.25	0.10	10.91	0.087	0.038	0.367
Sheerness	1.25	35.25	0.035	0.09	0.06	6.41	0.062	0.019	0.188

TABLE IV: Relevant statistical parameters for applicability of the superstatistical model to differences of observed non-tidal residuals at different locations. The short and the long time scales ( $\tau$  and  $T$ ) are expressed in hours. Parameters  $\tau$ ,  $T$  and  $\epsilon$  are described in Section II B.

### Acknowledgements

This research was supported by the EPSRC grant ‘Flood MEMORY’. The research was also supported in part by the National Science Foundation under Grant No. NSF PHY11-25915.

- 
- [1] C. Beck and E.G.D. Cohen, *Physica A* **322**, 267 (2003)
  - [2] C. Beck, E.G.D. Cohen, and H.L. Swinney, *Phys. Rev. E* **72**, 056133 (2005)
  - [3] H. Touchette and C. Beck, *Phys. Rev. E* **71**, 016131 (2005)
  - [4] P. Jizba, H. Kleinert, *Phys. Rev. E* **78**, 031122 (2008)
  - [5] P.-H. Chavanis, *Physica A* **359**, 177 (2006)
  - [6] S.A. Frank and D.E. Smith, *Entropy* **12**, 289 (2010)
  - [7] C. Anteneodo and S.M. Duarte Queiros, *J. Stat. Mech.* P10023 (2009)
  - [8] E. Van der Straeten and C. Beck, *Phys. Rev. E* **80**, 036108 (2009)
  - [9] C. Mark, C. Metzner, B. Fabry, arXiv:1405.1668
  - [10] R. Hanel, S. Thurner, and M. Gell-Mann, *PNAS* **108**, 6390 (2011)
  - [11] C. Tsallis, *J. Stat. Phys.* **52**, 479 (1988)
  - [12] C. Tsallis and A.M.C. Souza, *Phys. Rev. E* **67**, 026106 (2003)
  - [13] K. Briggs, C. Beck, *Physica A* **378**, 498 (2007)
  - [14] C. Beck, *Phys. Rev. Lett.* **98**, 064502 (2007)
  - [15] L. Leon Chen, C. Beck, *Physica A* **387**, 3162 (2008)
  - [16] A.Y. Abul-Magd, G. Akemann, P. Vivo, *J. Phys. A Math. Theor.* **42**, 175207 (2009)
  - [17] K.E. Daniels, C. Beck, and E. Bodenschatz, *Physica D* **193**, 208 (2004)
  - [18] C. Beck, *Physica A* **331**, 173 (2004)
  - [19] S. Rizzo and A. Rapisarda, *AIP Conf. Proc.* **742**, 176 (2004)
  - [20] D.N. Sobyenin, *Phys. Rev. E* **24**, 051128 (2011)
  - [21] P.D. Dixit, arXiv:1210.3015
  - [22] C. Tsallis, *Introduction to Nonextensive Statistical Mechanics*, Springer, 2009
  - [23] M.S. Santhanam and H. Kantz, *Phys. Rev. E* **78**, 051113 (2008)
  - [24] G.C. Yalcin, C. Beck, *Physica A* **392** 21 (2013)
  - [25] A. Porporato, G. Vico, P.A. Fay, *Geophys. Res. Lett.* **33**, L15402 (2006)
  - [26] J.A. Tawn, *J. R. Stat. Soc. Series C*, **41**, 1 (1992)
  - [27] M.A. Merrifield, M. E. Maltrud, *Geophys. Res. Lett.*, **38**, L21605 (2011)
  - [28] F. M. Calafat, D. P. Chambers, M.N. Tsimplis *J. Geophys. Res.*, **117**, C09022 (2012)
  - [29] S. Dangendorf, C. Muddersbach, T. Wahl, J. Jensen. *Ocean. Dyn.*, **63**, 209-224, (2013)
  - [30] S. Dangendorf, S. Mller-Navarra, J. Jensen, F. Schenk, T. Wahl, and R. Weisse, *J. Climate*, **27** (2014)
  - [31] K.J. Horsburgh, C. Wilson. *J. Geophys. Res.*, **112**, C08003 (2007)
  - [32] W. R. Peltier, *Ann. Rev. Earth. Planet. Sci.*, **32**, 111-149 (2004)
  - [33] G. Wöppelmann, C. Letetrel, A. Santamaria, M-N. Bouin, X. Collilieux, Z. Altamimi, S.D.P. Williams, B. Martin Miguez, *Geophys. Res. Lett.*, **36**, L12607 (2009)
  - [34] C. Cabanes, A. Cazenave, C. Le Provost. *Science*. **294**, 5543 (2001)
  - [35] I. Haigh, R. Nicholls, N. Wells. *Cont. Shelf Res.* **29**, 17 (2009)
  - [36] R. Pawlowicz, B. Beardsley, S. Lentz. *Comput. Geosci.* **28**, 8 (2002)
  - [37] C. Batstone, M. Lawless, J. Tawn, K. Horsburgh, D. Blackman, A. McMillan, D. Worth, S. Laeger, T. Hunt. *Ocean Eng.*, **71** (2013)

- [38] W. T. Eadie, D. Drijard, F.E. James, M. Roos, B. Sadoulet. Statistical Methods in Experimental Physics (1971)
- [39] British Oceanographic Data Centre. <http://www.bodc.ac.uk/>
- [40] C. Beck, Physica A 277, 115 (2000)